



RESEARCH ARTICLE

MECHANISM OF SOUND PROPAGATION IN SEAWATER

<sup>1</sup>Sakineh Akbari Nia and <sup>2,\*</sup>Mehdi Delphi

<sup>1</sup>Department of Physics, Shoushtar Branch, Young Researchers Club, Islamic Azad University, Shoushtar, Iran

<sup>2</sup>Department of Civil Engineering and Water, Shoushtar Branch, Islamic Azad University, Shoushtar, Iran

ARTICLE INFO

Article History:

Received 2<sup>nd</sup> July, 2011  
Received in revised form  
14<sup>th</sup> August, 2011  
Accepted 18<sup>th</sup> September, 2011  
Published online 15<sup>th</sup> October, 2011

Key words:

Sound propagation,  
Sea, sonar system,  
Reflection, processing.

ABSTRACT

Sound wave similar to other mechanical waves needs an environment to propagate. Speed of sound wave is about 331.4 (m/s) in air and this value is between 4.5 to 5 times the above value for seawater. Speed of sound in salt sea water depends on temperature, salinity and pressure. Sound propagation in seawater has many applications such as preparing photos of bottom topography, hydrography and appointing the water properties in sea (temperature, salinity, and so on ) etc. It has applications in fisheries, marine mapping, navy force, shipping and other researches and marine activities too. Propagation of sound pulses and signals and variations of sound speed in salt sea water follow the acoustical wave equation. In this paper, mechanical mechanism of sound propagation underwater in Pacific Ocean.

Copy Right, IJCR, 2011, Academic Journals. All rights reserved

1. INTRODUCTION

The ocean is a random medium having both deterministic and nondeterministic characteristics. This behavior often leads to difficulty in performing such underwater applications as telemetry and tomography. These applications require high bit rates, low error probability and long distance capabilities which are extremely difficult to achieve, given the ocean is a highly complex medium (Baggeroer, 1984). The ocean acoustic channel creates strong amplitude and phase fluctuations in acoustic transmissions. These fluctuations can be induced by internal waves, turbulence, temperature gradients, density stratification or by other related phenomena that cause local perturbations in the sound speed. Perturbations interact with the regular wave fronts through diffractive and refractive effects, causing temporal, spatial, and frequency-dependant fluctuations in the received waveforms, there are also multiple propagation paths from transmitter to receiver for most underwater propagation geometries (Catipovic, 1990). Received signal fluctuations arise from these medium fluctuations and cause the signal to oftentimes become unreadable. These underwater acoustic communications systems rely heavily on having prior knowledge of the underwater acoustic environment. Predictions of pulse behavior may also aid in developing smoothing or filtering techniques of the waveforms. This information will directly impact the optimality of receiver design, as well as the actual information rate that the underwater channel can support (Gendron, 2005).

2. Matched-field Processing

In recent years, researchers have suggested an important improvement of the tomographic scheme. The deployment of an array of hydrophones as the measuring device instead of a single hydrophone unit makes applications to improve signal processing, such as matched-field techniques, more feasible (Taroudakis and Markaki, 1997). A broadband pulse is emitted from a spherical acoustic source (either moored or towed) and received by a vertical line array (VLA) of hydrophones, this is a typical setup for most modern acoustic propagation experiments.

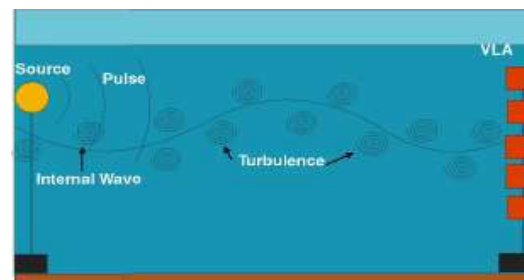


Fig. 1.2. : Schematic of underwater acoustic propagation experiment

A number of different approaches for processing received signals have been proposed; in general these methods utilize the information of the arrival pattern of the signal obtained in the time domain. Predictions of arrival patterns can be used for the classification of acoustic channels affected by varying

\*Corresponding author: [delfi.mehdi@gmail.com](mailto:delfi.mehdi@gmail.com)

turbulent environments. The travel times and arrival depths of these pulses are dependent on the encountered environmental parameters, i.e. turbulence and internal waves (Taroudakis and Markaki, 1997). Matched-field processing, involves "matching" the arrival pattern of a received signal to those of simulated candidate environments. The approach as described by Taroudakis and Markaki (1997) utilizes a reference environment defined by a simulation. The differences of the actual arrival times with respect to those predicted for the reference environment are calculated and define a linear inverse problem. These differences have a functional relationship with the actual environmental parameters with respect to those of the reference environment. The sound-speed function  $c(r,z)$  corresponding to the set of measured data can then be recovered (Taroudakis and Markaki, 1997). The temperature and depth fluctuations of the sound speed profile may indicate the presence of mesoscale eddies, mixing, and/or internal waves.

### 3. Quantification of Internal Waves and Turbulence

Characterizing the effect that fluctuations have on transmitted pulses is the goal of many researchers. However, sound pulses emitted at the sound channel axis encounter 0 Perturbations from both internal waves and small scale turbulence. Stewart (Stewart, 1969) commenting on the study of stably stratified turbulence wrote, [It is greatly complicated by the fact that we have two quite different types of flows intermingled: turbulence and internal gravity waves. In addition, the inferences that we should like to draw for the unmeasured aspects of the field are totally different for the two kinds of motion. Also there is the further complication of a nonlinear coupling that causes energy to flow between them...It is clearly desirable to be able to distinguish between the effects of turbulence and waves, but it is not clear that it is possible to do so. To the first question, I would reply that it is clearly desirable to attempt to ake the distinction. It is never possible to measure all the features of the particular field. One must measure some aspects and infer the rest. The inferences which would be drawn from a measurement of some aspects of a wave field should be quite different from the inferences drawn from similar measurements in turbulence field (Stewart, 1969). Since 1969, methods for quantifying turbulence have improved however there is still no exact means to discriminate between internal waves and turbulence. For instance, an internal wave packet of highly non-linear waves can grow regions of strong turbulence, this "breaking wave" is neither strictly wave nor strictly turbulence, but contains aspects of both (D'Asaro and Lien, 2000). It thereby becomes an impossible task to form a distinction between the two. Some flows however are more turbulent or more wavelike than others (D'Asaro and Lien, 2000). In general, internal waves are the dominant cause for temporal fluctuation during long range propagation (Tang and Tappert 1997). For short range propagation, these internal waves may break causing small scale turbulence and the dominance of one feature over the other is unknown (D'Asaro and Lien, 2000). Internal waves are assumed to dissipate and drive turbulence, this combination has been found to have a substantial effect on arrival time fluctuations during short range propagation (Heney *et al.*, 1997).

### 4. Environmental background

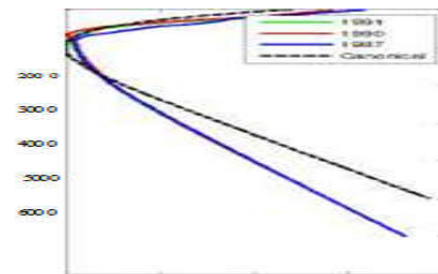
This paper presents an overview of the complexity of the ocean acoustic environment, which is necessary for understanding the theoretical approach of the computational model.

### 5. Sound Velocity in Water

The sound speed in the ocean is an increasing function of temperature, salinity, pressure, and depth. The following is an empirical function for sound velocity,  $c$ , in terms of three independent variables: temperature -  $T$  ( $^{\circ}C$ ), salinity -  $S$  (parts1000), depth -  $z$  (m) (Brekhovskikh, 1982).

$$c = 1449.2 + 4.6T - 0.055T^2 + 0.00029T^3 + (1.34 - 0.01T)(S - 35) + 0.016z \quad (1)$$

Oceanographers perform CTD (Conductivity, Temperature, and Depth) scans of the ocean to determine the sound speed over a region. Figure 2-1 shows a plot of three sound speed profiles calculated using CTD data obtained from the National Oceanographic and Atmospheric Administration.



Pacific Ocean CTD scans (NOAA/EPIC, 2005).

Table 1: Date and location of CTD casts used for Figure 2-1 (NOAA/EPIC, 2005).

Latitude	Longitude	Date of CTD cast
165° 0.3 E	24° 0.5' N	04 August 1987
158° 0.6' W	22° 47.1' N	24 July 1990
158° W	22° 45.0' N	09 July 1991

### 6. Detecting turbulence intensity by sound propagation

Sending sound signals having known correct and appropriate frequency underwater in sea appoints its application, therefore the main purpose of acoustical detecting would be found in optimum. Velocimetry is an applied usefulness of sound propagation underwater in sea. A typical feature of a turbulent flow, is that the fluid velocity fluctuates significantly and irregularly over space and time (Pope, 2001). Figure 3 illustrates fluid velocity fluctuations over time in a turbulent ocean.

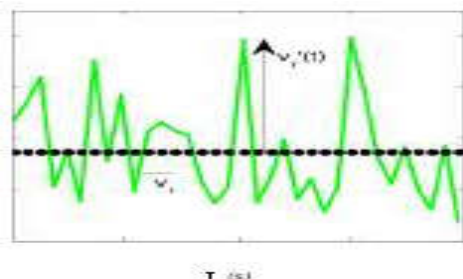


Figure 4.1. Turbulent velocity fluctuations

## 7. Turbulence Spectrum

As mentioned previously, a random field is statistically stationary if all statistics are invariant under a shift in time. Similarly, the field is statistically homogeneous if all statistics are invariant under a shift in position. For homogeneous turbulence, the spectra remain the same in both the temporal and spatial domains (Tennekes and Lumley, 1972). If the field is also statistically invariant under rotations and reflections of the coordinate system then the field is isotropic and is analyzed using the Kolmogorov spectrum for isotropic turbulence in the spatial domain.

## 8. Kolmogorov Spectrum

In 1941, A. Kolmogorov postulated that the one-dimensional energy spectrum  $E(k)$ , within the inertial sub range can only depend on length scale, measured by wave number  $k$ , and dissipation rate  $\varepsilon$ , and through dimensional analysis arrived at the famous Kolmogorov - 53 spectrum as a function of vortex size. This spectrum has a slope of  $k^{-5/3}$ .

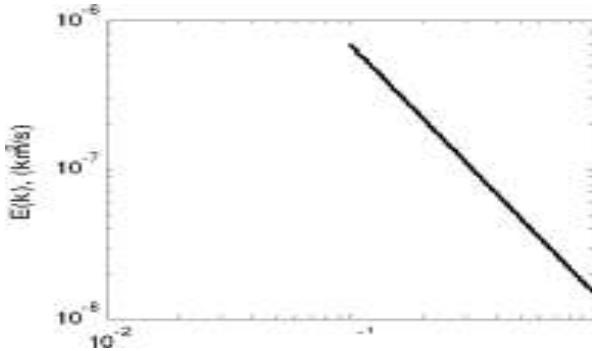


Fig. 4.3. Kolmogorov Spectrum  $E(k)$ , Inertial Subrange.

The Kolmogorov hypothesis can be developed to form a model energy spectrum for all wave numbers, including the energy-containing sub range and the dissipation sub range.

## 9. Garrett-Munk Spectrum of Internal Waves

The internal wave spectrum in the deep ocean has consistently the same shape wherever it is observed, except when the observations are made close to a strong source of internal waves (Lvov and Tabak, 2001). Based on these field observations, Garrett and Munk (1979) developed an energy-frequency spectrum, known as the Garrett-Munk spectrum of internal waves, Figure 4. In Figure 4, the wave frequency is plotted on the x-axis in cycles per hour (cph) and the energy per wave frequency ( $m^2 cph$ ) is plotted on the y-axis. Internal waves evolve over a wide spectrum of frequency scales, depending on their wavelength. In internal wave spectrum below, the buoyancy frequency is the upper limit of wave frequencies, so that can propagate through a system. The lower limit of internal wave frequencies is the Coriolis or inertial wave frequency,  $f$ . The inertial frequency is defined as  $f = 2Q \sin p$ , where  $Q$  is the angular velocity of the earth's rotation and ( $p$  is the latitude. At low latitudes, wave motions become inertial oscillations, where particles have horizontally circular trajectories (Wadzuk and Hodges,

2004). The following is the empirical expression for spectral energy as proposed by Garrett and Munk:

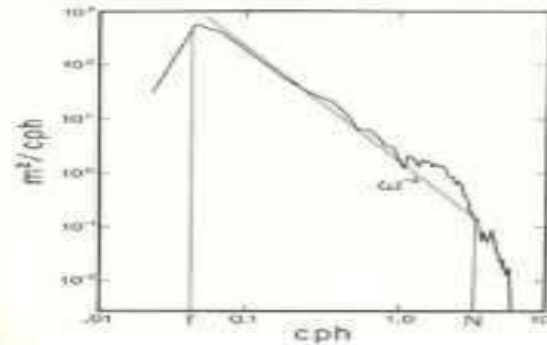


Figure 4.5: Garrett-Munk Spectrum of Internal Waves,  $E(\omega)$

$$E(k,m) = 2fNE(\text{mm}^*) \quad (2)$$

Where  $E$  is a constant quantifying the total energy content of the internal wave spectrum,  $N$  is the buoyancy frequency,  $f$  is the Coriolis parameter,  $k$  and  $m$  are the horizontal and vertical components of the wave vector respectively, and  $m^*$  is a reference vertical wave number to be determined from observations.

## 10. Some acoustical simulations of phenomena underwater

### 10.1. Comparison of Measured and Simulated Turbulence

The strategy used here is to populate the fluid with a finite number of two-dimensional vortices of random strengths and of random locations. Location is chosen to be within the region of the sound channel axis and specified range of propagation. The eddy dimensions,  $r$  and  $v$ , are necessary for calculating the circulation values. The eddy radius,  $r_{\text{ortex}}$ , is chosen to be typical to the defined length scales of inertial and lower portion of the energy containing subrange and average circulations values for eddies of this size are a few  $\text{cm}^2/\text{s}$ , the eddy velocity  $v_{\theta}$  is thereby chosen accordingly, (NOAA,1997). The range of these values is listed in Table 6-1. The acoustic ray propagates through the induced velocity field of the vortices and is therefore affected by the "turbulence" generated by the vortices. It is the intention here to represent the ocean as realistically and accurately as possible, therefore comparison of simulation to those of experimentally measured velocities is necessary. D'Asaro and Lien (2000), took measurements in August and September of 1995, of the  $u$  and  $v$  induced fluctuating velocities from turbulence in the Knight Inlet in British Columbia, using a Lagrangian method. A Lagrangian method is neither strictly spatial nor temporal, but retains properties of both. The inlet is 100 km long, 3 km wide, and is strongly stratified by freshwater from the Klinaklini and contains a large amount of stratified turbulence comparable to the mixed turbulence found in the thermocline of the ocean (D'Asaro and Lien, 2000). This study does also consider measurements of turbulence from the thermocline from the northeast Pacific Ocean taken in February 1993 and 1995 to serve as a comparison between the stratified and mixed layer turbulence (D'Asaro and Lien, 2000). Figure 6 illustrates spectrum of the  $u$  and  $v$  velocity components in the frequency domain for the 29 measurement trajectories; each color corresponds to the flow region where the data was measured. This spectrum peaks at an energy on the order of

$10^3 m^2 s^{-1}$  and the majority of activity pertains to a frequency range on the order  $3 \times 10^{-1} < \omega < 10^{-1}$ . The  $\omega$  seen here is identical to our frequency variable.

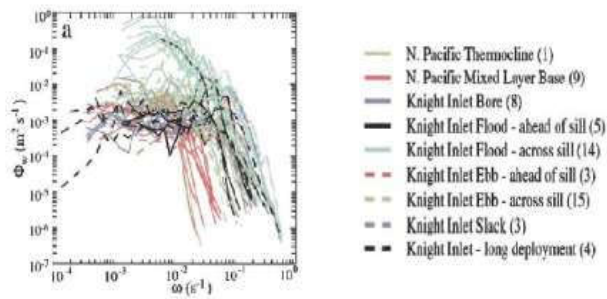


Fig. 6.31. Energy spectrum of the  $u$  and  $v$  fluctuating velocity components measured from the Knight Inlet (D'Asaro & Lien, 2000).

From this spectrum, two simple idealized shapes can be formed. Figure 7, on the left depicts a shape that is at first flat and constant and is then followed by a steep drop off; this is consistent for the turbulence measured in the inlet flow. Thermo cline velocities produce a smoother decreasing curve, seen on the right in Figure 7. These idealized shapes are used as comparison for the simulated spectra, which is taken in the wave number domain. This comparison is appropriate because the flow is considered homogenous and as mentioned earlier, spectral for homogeneous turbulent flow is identical in the spatial and temporal domains (Tennekes and Lumley, 1972). The measured velocities are again Lagrangian, and therefore their spectra would exhibit similar properties in wave number space.

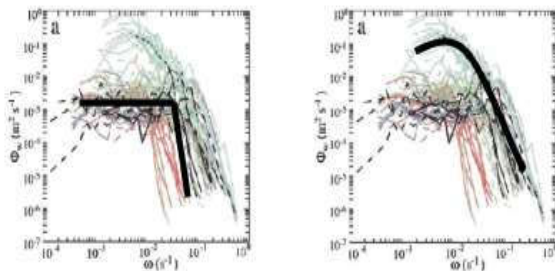


Fig. 6.32. LEFT: Shape of flows in inlets. RIGHT: Shape of flows in Thermo cline

The simulated turbulence is constructed over a propagation distance of 10km. The flow is observed over 30 realizations, each realization corresponding to 10s of geophysical time for a total sample 300s. Each vortex is conducted with the ambient current taken as  $U_x = 0.0005$  kms, and is considered "frozen" during the passage of the sound pulse, since the propagation time of the acoustic pulse is short compared to the fluid motion (Weber, 2003). The velocity at any point,  $P$ , will vary in time. The perturbation strength of the eddy field is the ratio of the average r.m.s. value of the  $u$  velocity to the ambient flow velocity, this strength should be typically about 10%. The number and strengths of the vortices are adjusted to results in turbulence intensity of about 10% and to produce spectra similar to those of Figure 6-31. Meanwhile some eddies are observed in the basin including turbulence. 25 of these eddies observed are shown in the following figure and then simulating them by using turbulence closure in solution of shallow water equation

in MATLAB resulted in the second figure for horizontal(H) and vertical(V) components of velocity in a good consistence with measurements and observations.

## 11. Summary and Discussion

The ocean acoustic channel creates strong amplitude and phase fluctuations in acoustic transmissions (long range and short range) used for underwater communications. These fluctuations can be induced by internal waves, turbulence, temperature gradients, density stratification or by other related phenomena that cause local perturbations in the sound speed. Received signal fluctuations arise from these medium fluctuations and cause the signal to oftentimes become unreadable. Underwater acoustic communications systems rely heavily on having prior knowledge of the underwater acoustic environment. The ocean is a stratified medium containing several layers. The layer of interest is the thermocline, which hosts a large temperature gradient and thereby a region where the sound speed is at a minimum, the sound channel axis. The sound channel axis acts as a waveguide, sound speed increases linearly toward the ocean floor and increases exponentially toward the ocean surface. The ocean's sound speed is a function of depth, salinity, and temperature. It is represented by the canonical profile developed by Munk (1974), which accounts for the mentioned variability. Profile parameters were taken from the long range propagation experiment, the SLICE89. The governing equations for the acoustic propagation model were derived from the wave equation which is simplified to the eikonal equation. The solution of the eikonal equation describes the behavior of ray trajectories and the travel time along them. For guided wave propagation the range can be viewed as the "time-step" variable, and the solution to the eikonal equation can be reduced to that of Hamiltonian form, known as the one-way ray equations, a set of second-order nonlinear differential equations.

### 11.1. Long Range Propagation

For long range propagation, transmission through an internal wave field is considered; this environment has been shown to cause ray chaos and associated stochastic properties. Previous models consider these nondeterministic effects and deterministic effects individually. This internal wave model accounts for both by representing the field as a harmonic function with randomly perturbed phase and/or amplitude by additive Gaussian white noise. Numerical analysis served as a means to justify our internal wave model and to demonstrate that the addition of random fluctuations leads to different characteristics in the acoustic arrivals during long range propagation, where it is believed that internal waves are the dominant source of acoustic fluctuations (Tang and Tappert 1997). The effect of noise intensity on chaotic ray behavior was examined through the construction of bifurcation and phase diagrams, Poincare maps, and maximum propagation range and time front plots. It was demonstrated that long range wave propagation behaves differently in the presence of imperfectly periodic internal waves. Bifurcation diagrams verified the various regimes of sound ray behavior, showing that addition of random phase modulation results in almost immediate ray divergence. These imperfect internal waves also cause the distortion of

Poincare sections for a non-chaotic environment. In a chaotic environment the diagrams appear stable; it is the stochastic properties of this internal wave model that cause instability. Time front plots demonstrated the multi-path structure that occurs in the ocean channel. The smearing of this predicted the arrival structure in the tail end of the time front plots suggests the development of micro-folds and micro-caustics which significantly complicate the identification of signals. This study of 1000km range undisturbed underwater sound propagation has revealed that random phase fluctuations are responsible for poor propagation, indiscernible arrival structure, and in some cases surface intersection. This behavior is highly dependent on the intensity of the stochastic perturbations.

### 11.2. Short Range Propagation

Short range ray propagation was investigated using three simulated turbulence environments: internal waves, simulated eddy turbulence, and the combination of internal waves and eddy turbulence. Each vortex in the eddy field was characterized by two-dimensional potential vortex, with randomly assigned strength and location within the region of the sound channel axis and 10km propagation range. The number and strengths of the vortices resulted in a turbulence intensity of about 10%. Internal waves were represented by the imperfectly harmonic forcing function. A numerical study was done over two initial launch angles of  $\phi(0) = 7.5^\circ$  and  $0^\circ$ , using both a stable and chaotic internal waves and a consistent eddy field for all simulations. The following conclusions are made based on predicted arrival structure observed from the time front branch. The internal waves supply the majority of variation in arrival depth. The turbulent eddy field is primarily responsible for delay fluctuation. The combination environment hosts both fluctuations. The amount of ray path degradation is dependent on the intensity of the internal waves. The amount of temporal fluctuation is dependant of the location of eddies and initial launch angle. One motivation for these simulations was to determine if there were any trends in the energy-frequency spectra that were common to each perturbation scenario, in order to provide a means to separate each contribution from the combination environment. The spectra of fluctuating MTV at 10km over time offered no clear distinction for this separation. However, it can be concluded that the internal waves are the dominant perturbation observed in the spectra. This observed internal wave dominance is dependent on the intensity of the wave.

It has been demonstrated that the predicted arrival patterns of rays traveling through ocean turbulence for long and short range propagation are dependent on initial conditions, intensity of the perturbations, and propagation distance. The results of these reference environments can serve as a prediction tool for transmitted signal behavior during underwater communication applications as well as the optimization of signal filters and hydrophone apertures.

## 12. REFERENCES

- Baggeroer, A. 1984. Acoustic Telemetry - An Overview. *Ieee Journal of Ocean Engineering*, OE-9(4), 229-235.
- Brekhovskikh, L. 1982. *Fundamentals of Ocean Acoustics* (G. Ecker, Ed.). Berlin, Germany: Springer-Verlag.
- Catipovic, J. 1990. Performance Limitations in Underwater Acoustic Telemetry. *Ieee Journal of Ocean Engineering*, 15(3), 205-216.
- D'Asaro, E. and Lien, R. 2000. Lagrangian Measurements of Waves and Turbulence in Stratified Flows. *Journal of Physical Oceanography*, 30, 641-654.
- Gendron, P. 2005. Estimating mutual information for the underwater acoustic channel. Manuscript in preparation, Naval Research Laboratory, Washington, DC.
- Lvov, Y. and Tabak, E. 2001. Hamiltonian formalism and the Garrett-Munk spectrum of internal waves in the ocean. *Prl*, 87, 1-5.
- Munk, W. 1974. Sound Channel in an exponentially stratified ocean, with application to SOFAR. *Journal of the Acoustical Society of America*, 55(2), 220-226.
- Stewart, R. 1969. Turbulence and waves in a stratified atmosphere. *Radio Scientific*, 4, 1269-1278.
- Tang, X. and Tappert, F. 1997. Effects of Internal Waves on Sound Pulse Propagation in the Straits of Florida. *Ieee Journal of Ocean Engineering*, 22(2), 245-255.
- Taroudakis, M. and Markaki, M. 1997. On the use of matched-field processing and hybrid algorithms for vertical slice tomography. *Journal of the Acoustical Society of America*, 102(2-1), 885-895.
- Tennekes, H. and Lumley, J. 1972. *A First Course in Turbulence* (1st ed.). Cambridge, MA: The MIT Press.
- Weber, F. 2003. Ultrasonic Beam Propagation in Turbulent Flow. Unpublished PhD Dissertation, Worcester Polytechnic Institute, Wor

\*\*\*\*\*